Correspondence to:
R. L. Jackson,
rebecca.jackson7@griffithuni.edu.au

AGU ADVANCING EARTH AND SPACE SCIENCE

Parameterizing the Impact of Seawater Temperature and Irradiance on Dimethylsulfide (DMS) in the Great Barrier Reef and the Contribution of Coral Reefs to the Global Sulfur Cycle

R. L. Jackson[1,2], A. J. Gabric[2,3], P. A. Matrai[4], M. T. Woodhouse[5], R. Cropp[1], G. B. Jones[6], E. S. M. Deschaseaux[6], Y. Omori[7], E. L. McParland[8,9], H. B. Swan[6], and H. Tanimoto[10]

[1]School of Environment and Science, Griffith University, Gold Coast, Queensland, Australia, [2]Australian Rivers Institute, Griffith University, Gold Coast, Queensland, Australia, [3]School of Environment and Science, Griffith University, Nathan, Queensland, Australia, [4]Bigelow Laboratory for Ocean Sciences, Maine, USA, [5]Climate Science Centre, Oceans and Atmosphere, Commonwealth Scientific and Industrial Research Organisation, Aspendale, VIC, Australia, [6]Centre for Coastal Biogeochemistry, School of Environment, Science and Engineering, Southern Cross University, Lismore, NSW, Australia, [7]Faculty of Life and Environmental Sciences, University of Tsukuba, Tsukuba, Japan, [8]Department of Marine and Environmental Biology, University of Southern California, Los Angeles, CA, USA, [9]Now at Department of Marine Chemistry and Geochemistry, Woods Hole Oceanographic Institution, Woods Hole, MA, USA, [10]Center for Global Environmental Research, National Institute for Environmental Studies, Tsukuba, Japan

Abstract Biogenic emissions of dimethylsulfide (DMS) are an important source of sulfur to the atmosphere, with implications for aerosol formation and cloud albedo over the ocean. Natural aerosol sources constitute the largest uncertainty in estimates of aerosol radiative forcing and climate and thus, an improved understanding of DMS sources is needed. Coral reefs are strong point sources of DMS; however, this coral source of biogenic sulfur is not explicitly included in climatologies or in model simulations. Consequently, the role of coral reefs in local and regional climate remains uncertain. We aim to improve the representation of tropical coral reefs in DMS databases by calculating a climatology of seawater DMS concentration (DMS$_w$) and sea-air flux in the Great Barrier Reef (GBR), Australia. DMS$_w$ is calculated from remotely sensed observations of sea surface temperature and photosynthetically active radiation using a multiple linear regression model derived from field observations of DMS$_w$ in the GBR. We estimate that coral reefs and lagoon waters in the GBR ($\sim$347,000 km^2) release 0.03–0.05 Tg yr^{-1} of DMS (0.02 Tg yr^{-1} of sulfur). Based on this estimate, global tropical coral reefs ($\sim$600,000 km^2) could emit 0.08 Tg yr^{-1} of DMS (0.04 Tg yr^{-1} of sulfur), with the potential to influence the local radiative balance.

Plain Language Summary Coral reefs are important sources of biogenic sulfur through stress-induced emissions of dimethylsulfide (DMS). This volatile sulfur compound has potentially important implications for atmospheric aerosol formation and cloud microphysical properties. However, coral reefs are not accounted for in global DMS climatologies or in model simulations. Consequently, the importance of coral reef-derived DMS in local climate is uncertain. Here, a proxy for seawater DMS concentration in coral reefs is derived from field measurements taken in the Great Barrier Reef, Australia. This proxy is used to calculate a climatology of DMS flux from coral reefs to estimate the contribution to the global sulfur cycle.

1. Introduction

Aerosols and clouds play a key role in the Earth's radiative budget and climate. The influence of anthropogenic greenhouse gas (GHG) emissions on the radiative balance is relatively well understood and is estimated to have exerted an average global warming effect of 2.3 W m^{-2} over the industrial period (IPCC, 2014). Anthropogenic and natural aerosols offset this warming effect by −0.9 W m^{-2} (−1.9 to −0.1 W m^{-2}) through scattering of short-wave radiation and increasing the albedo, lifetime, and cover of clouds (Andreae, 1995; IPCC, 2014; Twomey, 1974). However, the radiative effects of natural aerosols and their role in climate is complex and less well understood. Approximately 45% of the variance in aerosol radiative forcing is derived

from uncertainties in the role of natural aerosol sources, including marine dimethylsulfide (DMS) (Carslaw et al., 2013).

DMS is a volatile sulfur compound produced in the ocean by marine planktonic and benthic algae (Stefels, 2000), giant clams (Guibert et al., 2020; Hill et al., 2000), coral endosymbiotic dinoflagellates, and corals (Broadbent et al., 2002; Jones et al., 1994; Raina et al., 2013). The marine precursor of DMS, dimethylsulfoniopropionate (DMSP) has a range of hypothesized biological and ecological functions (McParland & Levine, 2019; Stefels, 2000), including a physiological stress response (Sunda et al., 2002). DMSP catabolism is mediated by algal and microbial processes. DMSP cleavage to DMS occurs via DMSP-lyase enzymes present in free-living and coral-associated endosymbiotic algae and microbes (Bullock et al., 2017). The DMSP demethylation pathway is a microbial process by which marine microbes convert DMSP into methanethiol (Bourne et al., 2016; Bullock et al., 2017; Raina et al., 2009). A portion (~10%) of the dissolved DMS (DMS$_w$) pool is ventilated to the marine boundary layer where it is rapidly oxidized to various sulfate aerosol precursor compounds (Andreae & Crutzen, 1997; Berndt et al., 2019; Veres et al., 2020).

Field observations and model simulations have identified a significant influence of DMS-derived sulfates on aerosol formation and growth, cloud condensation nuclei (CCN), and cloud droplet radius over the ocean (Gabric et al., 2013, 2018; Korhonen et al., 2008; Lana et al., 2012; Sanchez et al., 2018). DMS accounts for 18–43% of the global annual mean nonsea salt sulfate (nss-SO$_4$) aerosol burden (Gondwe et al., 2003; Kloster et al., 2006), exerting a top-of-atmosphere radiative forcing of -1.79 W m^{-2} (Mahajan et al., 2015) to -2.03 W m^{-2} (Thomas et al., 2010). However, regional variability in the importance of DMS in aerosol and cloud properties is evident, with the greatest sensitivity occurring over remote oceans where the influence of anthropogenic aerosol emissions is minimal (Fiddes et al., 2018; Woodhouse et al., 2013).

The Great Barrier Reef (GBR), Australia, has been recognized as a significant source of DMS, with the potential to influence local climate in NE Australia (Jackson et al., 2020; Jones et al., 2018). *Acropora* spp. are dominant throughout the Indo-Pacific and produce amongst the highest reported individual concentrations of dimethylated sulfur compounds (Broadbent et al., 2002; Jones et al., 1994; Swan et al., 2017a). Early field surveys found that aerosol concentration was significantly higher in the marine atmosphere directly over the GBR, compared to the seaward side (Bigg & Turvey, 1978). More recent field surveys have observed nucleation events occurring over the GBR (Leck & Bigg, 2008), where newly nucleated aerosol particles consisted of ~40% organic matter and ~60% sulfates, which are likely derived from DMS (Modini et al., 2009). Furthermore, there is a strong seasonal increase in fine-mode aerosol loading in spring and summer throughout the GBR, that has been observed from both field (Leck & Bigg, 2008) and satellite observations (Cropp et al., 2018; Jackson et al., 2018). This increase in fine-mode aerosol implies a temperature or irradiance-dependent biogenic influence (Christiansen et al., 2019; Korhonen et al., 2008; Long et al., 2014).

In corals, DMSP biosynthesis and cleavage to DMS is upregulated in response to oxidative stress caused by exposure to high sea surface temperature (SST), irradiance (Deschaseaux et al., 2014b; Fischer & Jones, 2012; Jones et al., 2007; Swan et al., 2017b), and low salinity (Gardner et al., 2016). Oxidative stress is caused by the release of reactive oxygen compounds (ROS) by coral cell mitochondria and zooxanthellae photosystems which can damage cells, tissues, and DNA (Lesser, 2011; Weis, 2008). Irradiance stress can be exacerbated in corals during aerial exposure at low tide (Buckee et al., 2020), with DMS being released directly to the atmosphere and resulting in measured spikes in atmospheric DMS (DMS$_a$) of up to 45.9 nmol m^{-3} (1,122 ppt) which can persist for around 8 h (Swan et al., 2017b). This is well above typical oceanic emissions of ~4–8 nmol m^3 (~100–200 ppt) (Kettle et al., 1999).

The rate of photosynthesis in coral-associated zooxanthellae increases linearly with photosynthetically active radiation (PAR) until photosystems become saturated and a maximum rate is achieved (Anderson et al., 1995; Gorbunov et al., 2001; Winters et al., 2003). For PAR beyond this maximum light threshold, photoinhibition occurs and excess light energy is dissipated as heat via various photoprotective mechanisms (Gorbunov et al., 2001; Melis, 1999). Excess light energy is quantified as excess excitation energy (EEE) and when not all EEE is dissipated as heat, photodamage can occur to Photosystem II (PS II), inhibiting the transport of electrons and damaging protein structure. When the rate of photodamage exceeds that of photoprotective repair, photodamage accumulates, and ROS are released into coral tissues (Lesser, 2011;
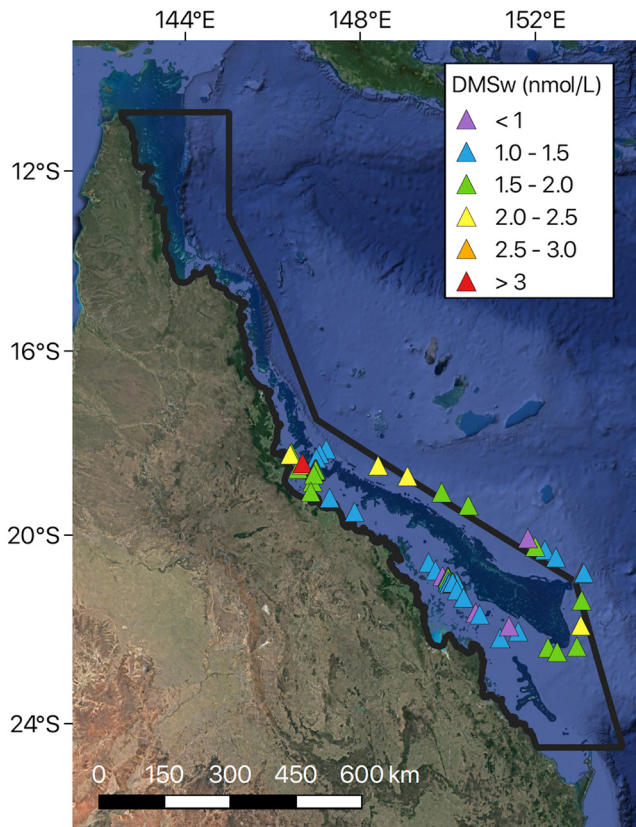
Figure 1. Map of northeast Queensland, Australia, showing the boundary of the Great Barrier Reef Marine Park (black outline) and DMS_w sampling locations and daily mean concentration during RV *Investigator* voyage IN2016_V05. Satellite imagery © Google Earth 2020. DMS_w, dimethylsulfide concentration.

Weis, 2008). If conditions persist, corals will expel their zooxanthellae and become bleached (Downs et al., 2002; Lesser, 2011; Yakovleva et al., 2009). High SST can exacerbate photodamage by further reducing the PAR absorption capacity (Jones et al., 2000, 2002).

DMS(P) readily scavenge ROS, thereby raising the coral oxidative stress threshold (Jones & King, 2015). ROS scavenging by DMS(P) produces dimethyl sulfoxide (DMSO), which can be reduced by bacteria and algae to DMS (Spiese et al., 2009). The concentration of DMS in coral reef waters is therefore dependent on the rate of DMS(P) (O) biosynthesis, which is related to coral oxidative stress (Deschaseaux et al., 2014b; Gardner et al., 2016; Raina et al., 2013). However, when oxidative stress exceeds coral physiological tolerance thresholds, ROS scavenging, and DMS(P) oxidation to DMSO increases, resulting in a decline in ambient DMS concentration (Deschaseaux et al., 2014a; Fischer & Jones, 2012). For example, Fischer and Jones (2012) found that when *Acropora* spp. were exposed to SST ~2 °C above ambient temperatures (26 °C), and PAR >6 mol m^{-2} h^{-1}, concentrations of DMS_a declined by ~90%. Similarly, Jones et al. (2007) demonstrated a decline in DMS_w of ~50% prior to a mass coral bleaching event in the central GBR when SST was >30 °C. The decrease in DMS_w was likely due to enhanced biochemical oxidation of DMS(P) to DMSO and/or a decline in production due to coral bleaching (Fischer & Jones, 2012; Jones et al., 2007). Thus, DMS_w in coral reefs is often closely linked to coral oxidative stress.

Currently, global DMS climatologies do not explicitly account for coral-derived DMS and the local DMS climatology of the GBR is unknown (Kettle & Andreae, 2000; Lana et al., 2011; Land et al., 2014). Although global DMS_w climatologies do incorporate measurements made within or nearby to coral reef lagoons (see Kettle et al., 1999), only a small number of coral reef regions are included and interpolation techniques do not account for seasonally variable coral emissions or direct coral-atmosphere DMS flux during coral exposure to air at low tide. The sensitivity of local climate to coral reef DMS emissions cannot be accurately quantified in earth system models without an improved representation of the source strength of coral reef-derived DMS.

Here, we derive a proxy for sea surface DMS_w in coral reef waters, from field measurements of DMS_w and physical oceanic parameters taken during Marine National Facility RV *Investigator* voyage IN2016_V05 in the GBR. Jones et al. (2018) compiled DMS_w measurements from three decades of surveys in the GBR, including the RV *Investigator* data set, to estimate annual DMS sea-air flux. The same data set is used here to derive a proxy for DMS_w, which is then used to calculate a climatology of DMS_w and sea-air flux from the GBR. The results provide insight into the importance of coral reefs to the atmospheric sulfur budget; an important source which may be lost with ongoing coral bleaching and reef degradation.

2. Materials and Methods

2.1. In-Situ and Remotely Sensed Measurements

DMS_w and total DMSP ($DMSP_t$) concentrations were measured in the southern and central regions of the GBR from September 29 to October 22, 2016 during RV *Investigator* voyage IN2016_V05 (Figure 1). This data set was generously provided by Jones et al. (2018), where detailed sampling and measurement protocols can be found. Seawater samples were taken at subhourly to 5-hourly frequency at 0–5-m depth using the underway seawater system. Samples were either immediately analyzed for DMS_w or preserved with 10% hydrochloric acid for later onshore analysis of $DMSP_t$. DMS_w was measured with a purge and trap gas chromatograph (GC) fitted with a flame photometric detector (GC-FPD) up to October 14, at which point

the equipment was required for Conductivity-Temperature-Depth measurements. From October 14 to 22, DMS_w was measured with an Equilibrator Inlet-Proton Transfer Reaction Mass Spectrometer (EI-PTR-MS) (Kameyama et al., 2009; Omori et al., 2017), which yielded results in agreement with the GC-FPD (Jones et al., 2018). $DMSP_t$ concentration in 100 ml seawater was determined using a GC-mass spectrometer operating in Single Ion Monitoring mode as described in .Deschaseaux et al. (2018) DMS_w and $DMSP_t$ measurements had a detection limit of 0.1 pmol (Jones et al., 2018).

Field and laboratory experiments have demonstrated that DMS concentration in corals and reef seawaters is affected by SST, PAR (and water clarity), salinity, and tidal height (Gardner et al., 2016; Jones et al., 2007; Raina et al., 2013). These variables were therefore used as potential predictors of DMS_w in the GBR. Wind-driven mixing and phytoplankton dynamics also influence DMS_w (Broadbent & Jones, 2006; Gabric et al., 2008; Stefels, 2000) and are, respectively, represented through the inclusion of wind speed (WS) and chlorophyll-*a* (CHL) as a proxy for phytoplankton biomass.

The DMS_w (nmol L^{-1}) and $DMSP_t$ (nmol L^{-1}) measurements were provided by Jones et al. (2018). Corresponding underway measurements of SST (°C), incident PAR (mol m^{-2} h^{-1}), sea surface salinity (SSS: psu) and WS (m s^{-1}) were downloaded from the Commonwealth Scientific and Industrial Research Organisation (CSIRO) Marlin online repository (https://www.marlin.csiro.au). Diffuse attenuation coefficient (k490: m^{-1}) as a proxy for water clarity, and CHL (mg m^{-3}) were not available from in the in-situ GBR data set. Daily mean k490 and CHL were obtained from the Moderate Resolution Imaging Spectroradiometer (MODIS) sensor aboard the Aqua and Terra satellites. Daily total PAR (mol m^{-2} d^{-1}) was also downloaded at 0.04-degree (∼4 km) resolution for each survey location from NASA OceanColor (https://oceancolor.gsfc.nasa.gov). To account for light attenuation at the sea surface, MODIS total PAR was reduced by the corresponding k490 value for a depth of 5 m, which corresponds to the sampling depth of 0–5 m. Although many coral reefs reside at depths greater than 5 m, coral reef seawaters are generally well mixed due to tidal and wind-driven mixing (Davis et al., 2020; Middleton et al., 1994). Therefore, we assume that DMS_w concentrations in the upper 5 m are representative of the water column and are most important for calculating the DMS sea-air flux.

Tidal height was also provided with the DMS_w data set for 8 of the 24 survey days when the RV *Investigator* was close to the Slashers Reefs in the central GBR (18.5°S, 147°E). Jones et al. (2018) separated tidal height and corresponding DMS_w into rising and falling tides and analyzed each data set separately. Significant positive correlations were identified between DMS_w and both rising and falling tide height. These correlations reflected an increase in DMS_w as tides fell, followed by a second increase in DMS_w as tides rose (Jones et al., 2018), due to dissolution of DMS-rich coral mucous in tidal slack water (Hopkins et al., 2016). For this work, tidal data were not separated into rising and falling tides and consequently, there was no significant correlation between DMS_w and tidal height ($p > 0.05$, $n = 133$). Tidal height is more important for measurements of DMS_w in seawater directly over the shallow coral reef flat (Jones et al., 2018). Given that the RV *Investigator* sampled deeper coral reef lagoon waters (waters surrounding the coral reef platforms), tidal height was not included as a potential predictor of DMS_w in the GBR.

2.2. Correlation and Multiple Linear Regression

To identify the strongest predictors of DMS_w in the GBR, hourly ($n = 184$) and daily ($n = 24$) mean DMS_w was correlated with each variable. Graphical analysis determined DMS_w (1.4 ± 0.07 nmol L^{-1}), $DMSP_t$ (8.5 ± 0.6 nmol L^{-1}), total daily PAR at 5 m (49.2 ± 0.2 mol m^{-2} d^{-1}) and WS (6.6 ± 0.4 m s^{-1}) to be approximately normally distributed. Values in parentheses represent the mean ± two standard errors (SE). SST was left skewed due to the dominance of values above the mean (25.9 ± 0.09 °C). Incident PAR was right skewed due to the inclusion of nighttime data (2.7 ± 0.4 mol m^{-2} d^{-1}), as was SSS (35.5 ± 0.02 psu) and CHL (0.19 ± 0.01 mg m^{-3}) due to the dominance of values below the mean. A conservative significance level ($\alpha = 0.01$) was used to account for nonnormality and outliers which are common in environmental data. A multiple linear regression was then derived between DMS_w and the strongest predictor variables.

2.3. Estimating DMS$_w$ in the GBR

A climatology (2001–2019) of DMS$_w$ was calculated from satellite observations in the GBR using the multiple linear regression derived from the RV *Investigator* IN2016_V05 data set. Daily data for each predictor variable were downloaded from MODIS Aqua and Terra at 0.04-degree resolution for the GBR (9.5°S–25°S, 142°E−154°E) from NASA OceanColor (https://oceancolor.gsfc.nasa.gov). Given the high number of missing observations in the high-resolution MODIS data set, a 30-days moving average of each variable was used. All data beyond the Great Barrier Reef Marine Park (GBRMP) boundary defined in Figure 1 were excluded.

2.4. DMS Sea-Air Flux

To calculate DMS sea-air flux, instantaneous wind speed at 10 m (U_{10}: m s^{-1}) was derived every 3 h from ERA5 0.25-degree *u* and *v*-wind components (Copernicus Climate Change Service, 2019). Calculated DMS$_w$ and MODIS SST were regridded to a 0.25-degree resolution. DMS sea-air flux was then calculated from daily DMS$_w$, SST, and each U_{10} measurement. U_{10} was derived every 3 h to avoid underestimating DMS flux calculated from daily mean wind speed.

Sea-air gas exchange is calculated as the product of the total gas transfer velocity (K_w) and the concentration difference between the sea surface (C_w) and atmosphere (C_a) as follows: Flux = K$_w$C$_w$-C$_a$α, where α is the solubility of DMS (Liss & Slater, 1974). DMS concentration is typically orders of magnitude lower in the atmosphere than at the sea surface and so, C_a is assumed to be zero. The resulting simplified equation (Equation 1) calculates DMS sea-air flux (µmol m^{-2} d^{-1}) from K_w (cm h^{-1}) and C_w (nmol L^{-1}). This common assumption can lead to a global flux overestimation of up to 5% (Johnson et al., 2011)

$$Flux = K_w C_w \tag{1}$$

For this analysis, three parameterizations for K_w are used to provide a range of DMS flux estimates. The parameterizations of Goddijn-Murphy et al. (2012) and Nightingale et al. (2000) specify that the DMS transfer velocity increases linearly with U_{10} and provide a relatively high estimate of DMS sea-air flux. These two parameterizations were derived for carbon dioxide and are normalized to a Schmidt number of 660 for DMS (Sc$_{DMS}$). Goddijn-Murphy et al. (2012) assume that K_w is equivalent to the water-side transfer velocity (k_w) (Equation 2), which is normalized to the SST-dependent Sc$_{DMS}$ calculated as follows: Sc$_{DMS}$ = 2,674-147.12 SST+3.726 SST^2-0.038 SST^3 (Saltzman et al., 1993)

$$K_{w,660} = k_{w,660} = \left(2.1 U_{10} - 2.8\right)\left(Sc_{DMS} / 600\right)^{-0.5}. \tag{2}$$

For the parameterization of Nightingale et al. (2000), K_w is calculated as a function of both the water-side and air-side DMS transfer velocities. For this parameterization, k_w is also linearly related to U_{10} (Equation 3) and is normalized to the SST-dependent Sc$_{DMS}$ (Saltzman et al., 1993)

$$k_{w,660} = \left(0.222 U_{10}{}^2 + 0.333 U_{10}\right)\left(Sc_{DMS} / 600\right)^{-0.5} \tag{3}$$

Total DMS transfer velocity is then calculated using Equation 4 (McGillis et al., 2000; Nightingale et al., 2000). The atmospheric gradient fraction (γ_a) is defined by $\gamma_a = 1 / \left(1 + k_a / \alpha k_{w,660}\right)$ (McGillis et al., 2000), where α is the solubility coefficient for DMS (11.4 at 26 °C) and k_a is the air-side transfer velocity calculated as a function of U_{10} and the molecular weight of DMS and water as follows: $k_a = 659 U_{10} \left(62.13 / 18.02\right)^{-0.5}$ (Kondo, 1975)

$$K_{w,660} = k_{w,660}\left(1 - \gamma_a\right). \tag{4}$$

The third K_w parameterization suggests that the DMS gas transfer velocity decreases for wind speeds exceeding 10 m s^{-1} and provides a more conservative estimate of DMS sea-air flux (Vlahos & Monahan, 2009). The divergence of the DMS transfer velocity at high wind speeds (>10 m s^{-1}) is accounted for by including an attenuation of the Henry's Law constant (Vlahos & Monahan, 2009). For this parameterization, K_w

is calculated using Equation 5 as a function of both $k_w = 4 \times 10^{-4} + 4 \times 10^{-5}(U_{10})^2$ and $k_a = 0.2\,U_{10} + 0.3$ (Schwarzenbach et al., 1994; Vlahos & Monahan, 2009). The parameterizations for k_w and k_a are given in units of cm s^{-1} and are converted to cm h^{-1} in order to calculate the total DMS transfer velocity

$$K_{w,660} = \left(\frac{1}{k_w} + \frac{1}{k_a H_{atten}} \right)^{-1} \tag{5}$$

The attenuated Henry's Law constant for DMS (H_{atten}) is calculated using Equation 6, where H is the Henry's Law constant in seawater (0.089) (Przyjazny et al., 1983), ϕ_B is the surface area of bubbles under the sea surface given by $\phi_B = 0.09(U_{10} / 10)^3$ and C_{mix}/C_w is the solubility enhancement of DMS, calculated to be 40 from Vlahos and Monahan (2009)

$$H_{atten} = H / 1 + \phi_B \left(C_{mix} / C_w \right) \tag{6}$$

During coral exposure to air at low tide, DMS is directly released to the atmosphere from corals and the mucous layer which quickly forms on the coral surface upon exposure (Hopkins et al., 2016). Direct coral-atmosphere DMS exchange can result in large spikes of atmospheric DMS concentration (Hopkins et al., 2016; Jones et al., 2007; Swan et al., 2017b). However, coral aerial exposure is not currently accounted for in DMS sea-air flux calculations. In this study, we attempt to quantify total DMS emissions from the GBR by including a laboratory-based estimate of direct coral-atmosphere DMS flux. Hopkins et al. (2016) measured the rate of DMS$_a$ production from *Acropora horrida* periodically exposed to air. Coral nubbins were obtained from parent colonies sampled in the Indo-Pacific and an estimate of coral aerial exposure at Heron Island in the southern GBR was used (Hopkins et al., 2016), where extreme low tides expose corals for about 2 h on 6 days per month (Wild et al., 2004). Assuming a similar pattern of coral exposure across the GBR, and given that *Acropora* is the dominant coral genus, it was estimated that corals in the GBR exposed to air release 9–35 µmol m^{-2} d^{-1} (mean 22 µmol m^{-2} d^{-1}). A fraction of the mean flux estimate is added to Equation 1, depending on the percentage cover of coral reefs within each 0.25 × 0.25-degree grid. Swan et al. (2017b) observed that corals have the strongest influence on DMS$_a$ levels during winter when the background oceanic flux is relatively low. Adding a fixed estimate of coral-atmosphere DMS release to our flux estimate is consistent with these findings, as the percentage contribution of aerially exposed corals to DMS flux is higher in winter. These intermittent spikes can exceed 40 nmol m^{-3} (1,000 ppt) and persist for up to 8 h during low and rising tides (Swan et al., 2017b). Tidal range is higher in the far northern GBR (Jackson et al., 2018), which could affect the frequency and extent of coral exposure to air at low tide. Assuming direct coral-atmosphere DMS flux for only 2 h on 6 days per month is therefore a reasonable and possibly conservative estimate.

3. Results

3.1. Correlation Analysis

Hourly mean observed DMS$_w$ positively correlated with SST and WS, and negatively with SSS and instantaneous PAR (Table 1). Hourly mean DMSP$_t$ and CHL did not significantly correlate with DMS$_w$.

Correlation coefficients were also calculated using a daily mean of each variable ($n = 24$); however, no significant correlations occurred ($p > 0.01$). To reduce the variability in this limited data set, we also calculated correlation coefficients for a 3-day moving average of each variable ($n = 24$). This resulted in similar correlations as the hourly mean data set, which increased in strength due to reduced variability (Table 1). At this time scale, instantaneous PAR no longer significantly correlated with DMS$_w$ likely due to averaging out the diel cycle. However, daily total PAR from MODIS observations was strongly positively correlated with DMS$_w$, reflecting a relative increase in concentration for days when total irradiance was high. Wind-driven mixing contributes to DMS sea-air exchange, and changes in SST, SSS, nutrients, and phytoplankton dynamics, which can explain the positive correlation between hourly mean DMS$_w$ and WS. Three-day moving mean WS did not correlate with DMS$_w$, yet DMSP$_t$ strongly positively correlated with DMS$_w$ (Table 1).

Table 1
Pearson's Linear Correlation Between Hourly and 3-Day Moving Mean DMS_w and Predictor Variables

	Hourly mean ($n = 184$[a])		3-days moving mean ($n = 24$)	
3	r	p	r	p
SST	**0.29**	**<0.001**	**0.56**	**<0.01**
SSS	**−0.28**	**<0.001**	**−0.62**	**<0.01**
WS	**0.23**	**<0.01**	0.39	0.06
Instantaneous PAR	**−0.21**	**<0.01**	−0.19	0.37
Total PAR at 5 m[b]	**0.19**	**<0.01**	**0.57**	**<0.01**
$DMSP_t$	0.14	0.08	**0.63**	**<0.01**
CHL[b]	−0.08	0.26	−0.10	0.65

[a]Corresponding WS and $DMSP_t$ were not available for all DMS_w measurements. For hourly mean WS, $n = 183$ and for $DMSP_t$, $n = 169$. [b]Data are derived from remotely sensed observations. Significant ($p < 0.01$) correlations are in bold.

Significant relationships between 3-day moving mean DMS_w and potential predictor variables (SST, SSS, PAR at 5 m, and $DMSP_t$) are shown in Figure 2.
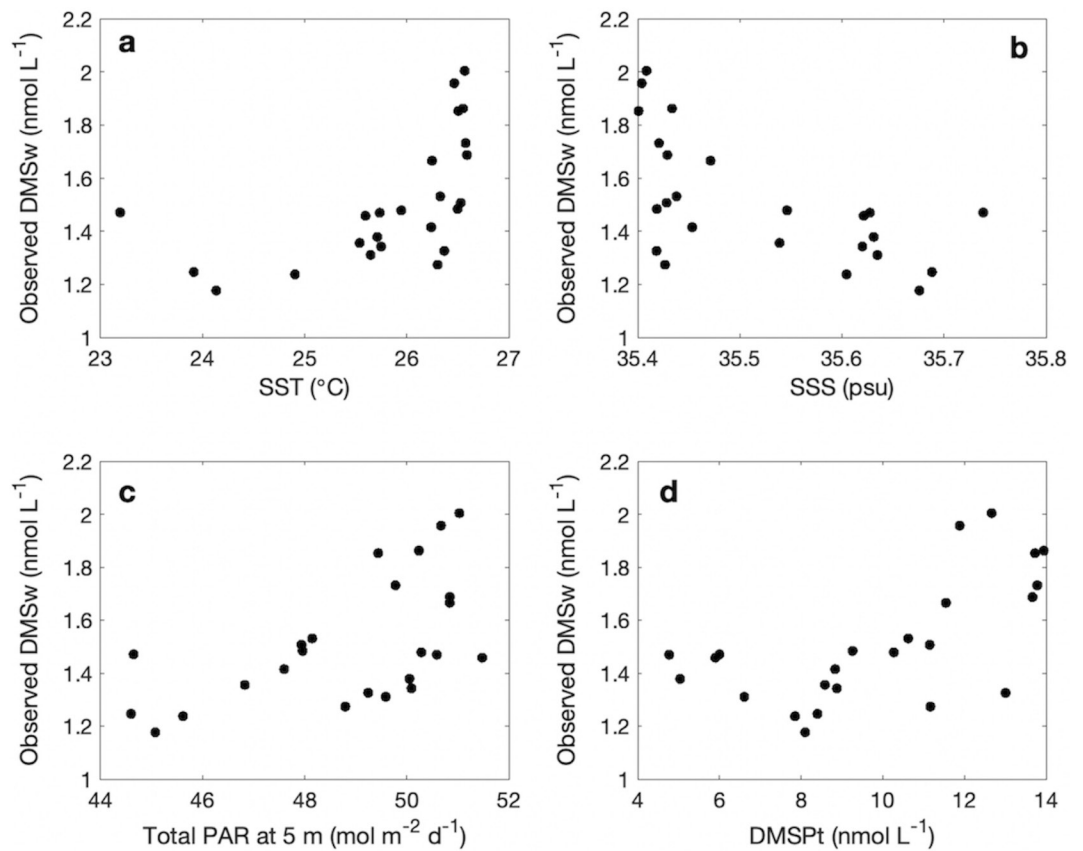

Figure 2. Relationship between 3-day moving mean observed DMS_w and (a) SST ($r = 0.56$), (b) SSS ($r = −0.62$), (c) total PAR at 5 m ($r = 0.57$), and (d) $DMSP_t$ ($r = 0.63$). DMS_w, dimethylsulfide concentration; SST, sea surface temperature; SSS, sea surface salinity; PAR, photosynthetically active radiation; DMSPt, total dimethylsulfoniopropionate.
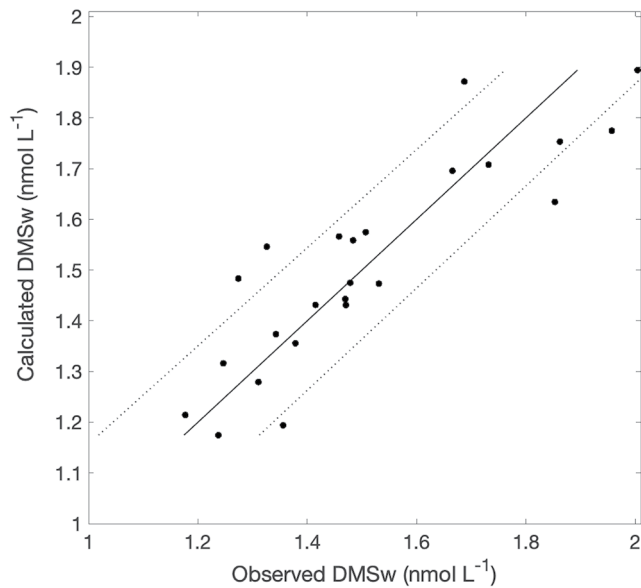
Figure 3. Observed vs. calculated DMS$_w$, showing the regression line (—) ± 95% confidence interval bounds (⋯). DMS$_w$, dimethylsulfide concentration.

3.2. Multiple Linear Regression

A multiple linear regression was derived from the 3-day moving mean data set (Equation 7). The resulting regression with standardized SST and total PAR as predictor variables explained 71% of the variance in observed DMS$_w$ (Figure 3; $r^2 = 0.76$, adjusted $r^2 = 0.71$, $p < 0.001$, $n = 24$). Quadratic terms were included to better reflect the observed relationships between DMS$_w$ and SST (Figure 2a) and PAR (Figure 2c). This ensured that the regression residuals were normally distributed, with equal variances across the range of calculated DMS$_w$. Removing these terms resulted in nonrandom residuals, indicating that the regression model was not reliable. Although SSS and DMSP$_t$ correlated with DMS$_w$ (Table 1), including these as predictor variables did not improve the regression. Including either SST or SSS with PAR as predictors resulted in an $r^2 > 0.6$. However, SST and SSS are strongly inversely correlated ($r = -0.9$, $p < 0.01$) and consequently, including both variables in the regression resulted in nonrandom residuals and a negative coefficient for SST, which does not reflect the relationship shown in Figure 2a

$$DMS_w = 0.10\,SST^2 + 0.34\,SST + 0.14\,PAR^2 + 0.12\,PAR + 1.28 \quad (7)$$

The parameterization of DMS$_w$ as a function of SST and PAR at 5 m is used to calculate DMS$_w$ in the GBR from remotely sensed observations. It is important to note that DMS$_w$ in coral reefs does not linearly increase with SST when coral thermal stress thresholds are exceeded (Fischer & Jones, 2012; Jones et al., 2007). To avoid overestimating DMS$_w$ for days when SST exceeded this threshold, SST in Equation 7 is substituted with an estimated coral thermal stress threshold.

The National Oceanic and Atmospheric Administration (NOAA) Coral Reef Watch define a coral thermal stress threshold as 1 °C above the SST of the climatologically hottest month of the year (Liu et al., 2006). This estimate is used to derive indices to predict coral bleaching (e.g., Degree Heating Weeks) and predict the extent and severity of coral bleaching events well in the GBR (Bainbridge, 2017; Hughes et al., 2018; Jackson et al., 2018; Skirving et al., 2018). These coral bleaching indices assume that living corals can tolerate summer PAR levels without bleaching (Skirving et al., 2018); however, when summer PAR combines with SST above the thermal stress threshold, coral bleaching (and a decline in DMS$_w$) can occur (e.g., Jones et al., 2007). Thus, for days when SST ≥ thermal stress threshold, DMS$_w$ was calculated from Equation 7, substituting SST for the coral thermal stress threshold. This threshold decreased with latitude, ranging from 27.5 °C in the southern GBR to 30 °C in the northern GBR. This reduced the average calculated DMS$_w$ in the GBR by ~0.01 nmol L^{-1} in late summer.

3.3. Climatology of DMS$_w$

A time series of DMS$_w$ in the GBR was calculated using Equation 7 from standardized MODIS observations of SST and total PAR at 5 m from 2001 to 2019. We assume that the empirical relationship derived between DMS$_w$, SST, and PAR at 5 m in the southern and central GBR can be used to estimate DMS$_w$ beyond the region and time frame for which Equation 7 was defined. It is recognized that this may not be an accurate representation of DMS$_w$ in the northern GBR or for other times of the year; however, in the interest of estimating total DMS$_w$ and flux, it is important to include an estimate of DMS$_w$ for the entire GBR and time period.

Calculated annual mean DMS$_w$ in the GBR was 1.5 nmol L^{-1}, ranging from an average of 1.2 nmol L^{-1} in winter to 1.9 nmol L^{-1} in summer, with little spatial variability (<0.1 nmol L^{-1}) (Figure 4). SST decreased with latitude and ranged from an average of 24 °C (20–26 °C) in winter to 27 °C (25.5–29 °C) in summer. Seasonal average PAR at 5 m ranged from 40 mol m^{-2} d^{-1} (35–44 mol m^{-2} d^{-1}) in winter to 50 mol m^{-2} d^{-1} (46–53 mol m^{-2} d^{-1}) in summer, decreasing with latitude in winter yet increasing with latitude in summer.
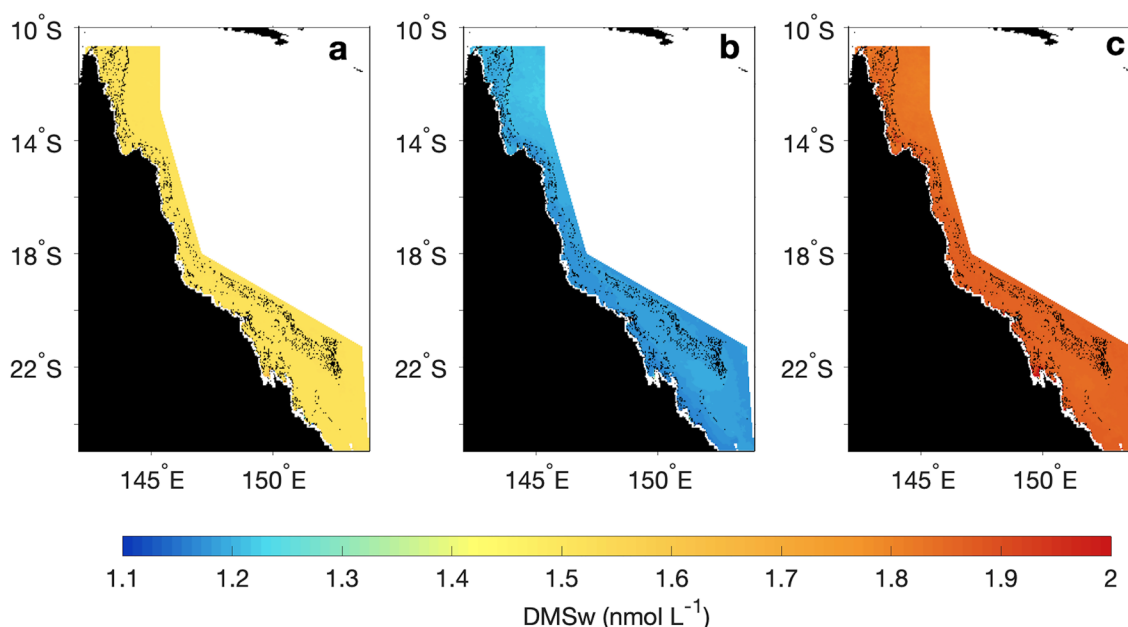
Figure 4. (a) Annual, (b) winter (May-October), and (c) summer (November-April) average calculated DMS$_w$ in the GBR. Northeastern Australia and the location of coral reefs in the GBRMP are shown in black. DMS$_w$, dimethylsulfide concentration; GBR, Great Barrier Reef; GBRMP, Great Barrier Reef Marine Park.

Although a small latitudinal gradient is evident in winter, with higher DMS$_w$ in the northern GBR due to higher SST and PAR, no clear latitudinal gradient is evident in the summer or annual mean DMS$_w$ concentration (Figure 4). This is due to the inverse meridional trends in summer SST and PAR, which resulted in uniform calculated annual and summer average DMS$_w$ (Figure 4). We assume that living corals and marine algae are adapted to the typical local environment and so uniform average concentrations can be expected throughout the GBR.

Calculated DMS$_w$ area-averaged over the GBR ranged from 1 ± 0.01 (2 SE) nmol L^{-1} in late winter to 2.1 ± 0.1 nmol L^{-1} in summer (Figure 5). Daily mean observed DMS$_w$ during the RV *Investigator* voyage was 1.5 ± 0.2 nmol L^{-1}, similar to mean calculated DMS$_w$ for the same time period and location (1.3 ± 0.04 nmol L^{-1}) (Figure 5a). The climatology of calculated DMS$_w$ shows a seasonal signal, with increased concentration in early summer (October-December), followed by a plateau in concentration in January-February when SST and PAR were highest and when coral bleaching typically occurs (Figure 5b).

3.4. Climatology of DMS Sea-Air Flux

DMS sea-air flux was calculated from MODIS observations of SST, U_{10} derived from ERA5 u and v-wind components and the DMS$_w$ time series (Figure 5a). Three parameterizations for K_w were used to calculate DMS sea-air flux and the mean of these is mapped in Figure 6. Annual mean DMS flux averaged over the GBR was 4.9 μmol m^{-2} d^{-1} (0.9–11.4 μmol m^{-2} d^{-1}), ranging from an average of 4.3 μmol m^{-2} d^{-1} (0.7–10.1 μmol m^{-2} d^{-1}) in winter, to 5.4 μmol m^{-2} d^{-1} (1.2–12.6 μmol m^{-2} d^{-1}) in summer (Figure 6). DMS flux remained consistently high over the coral reef, representing direct coral-atmosphere DMS exchange during coral exposure to air at low tide.

The climatologies of DMS sea-air flux area-averaged over the GBR show a seasonal signal, ranging from an average of 3.1 ± 0.3 μmol m^{-2} d^{-1} in late winter to 7.3 ± 1.6 μmol m^{-2} d^{-1} in late summer (Figure 7). Including an estimate of coral-atmosphere DMS release at low tide increased the GBR-averaged flux by 1.5 μmol m^{-2} d^{-1}. Nightingale et al. (2000) and Goddijn-Murphy et al. (2012) assume that sea-air flux increases linearly with U_{10}. However, Vlahos and Monahan (2009) suggest that the DMS gas transfer velocity decreases when wind speed exceeds 10 m s^{-1}, thereby providing a more conservative estimate of DMS sea-air flux (Figure 7). From the three DMS sea-air flux parameterizations (Figure 7), it is estimated that the
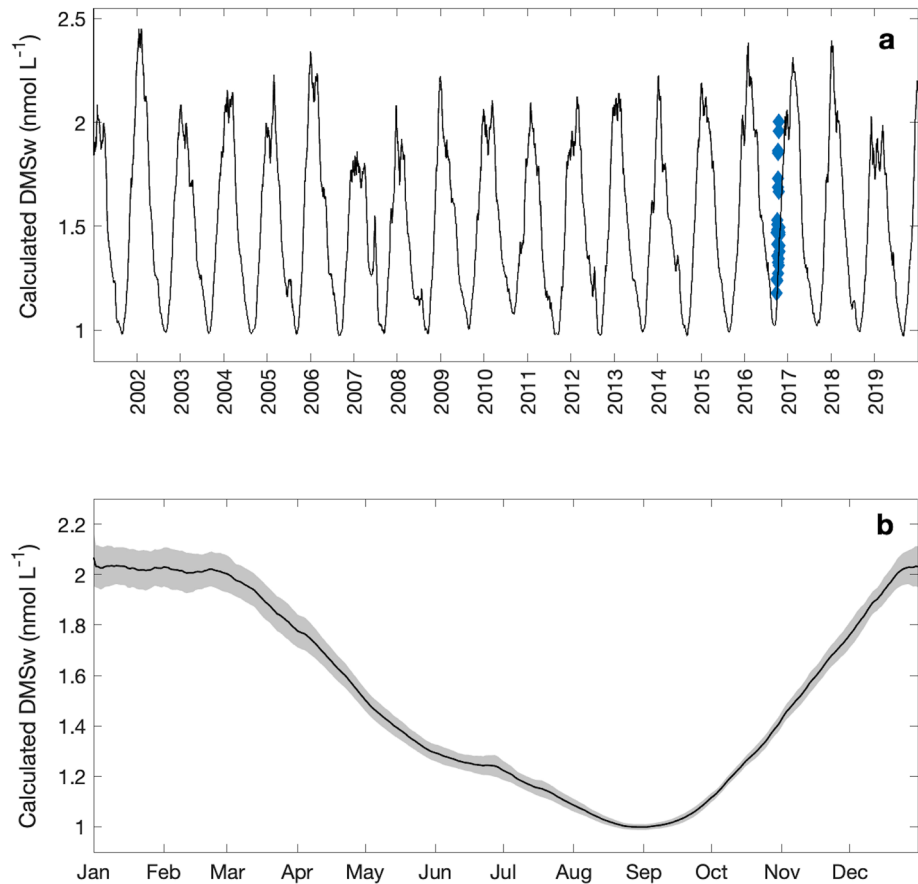
Figure 5. (a) Calculated DMS$_w$ averaged over the entire GBR from 2001 to 2019. Blue dots represent the daily mean observed DMS$_w$ in the southern GBR (~18°S–23°S). (b) Calculated DMS$_w$ climatology ±2 SE (shaded regions). DMS$_w$, dimethylsulfide concentration; GBR, Great Barrier Reef; SE, standard errors.

347,000 km^2 GBR and lagoon waters release 0.03–0.05 Tg yr^{-1} of DMS (1,500–2,100 mol km^2 yr^{-1}), which is equivalent to 0.02 Tg yr^{-1} of sulfur.

4. Discussion

SST and PAR synergistically impact coral physiological stress (Rosic et al., 2020) and were correlated with DMS$_w$ concentration in the GBR. Both field and laboratory analyses have demonstrated an increase in intracellular and dissolved DMS(P) production from corals and in reef seawaters in response to increasing temperature and solar irradiance (Deschaseaux et al., 2014b; Gardner et al., 2016; Jones et al., 2007), until a coral physiological tolerance threshold is approached (Jones et al., 2007, 2018).

DMS$_w$ negatively correlated with instantaneous PAR (Table 1), reflecting photo-oxidation of DMS(P) during the day (Gabric et al., 2008; Galí et al., 2013). Conversely, DMS$_w$ positively correlated with daily total PAR (Table 1), reflecting a relative increase in coral and algal DMS production with solar irradiance (Deschaseaux et al., 2014b; Jones et al., 2007). DMS$_w$ also increased with decreasing SSS, supporting previous findings that DMS(P) are involved in the coral hyposalinity stress response (Gardner et al., 2016). Hourly mean DMS$_w$ did not correlate with DMSP$_t$ (Table 1), perhaps indicating that cleavage of DMSP is not the rate-limiting process in DMS$_w$ production. DMS(P) removal mechanisms such as rapid photo-oxidation during the day, microbial consumption and vertical mixing in the water column can confound the relationship between DMSP and DMS at the sea surface, highlighting the complexity in DMS(P) cycling (Gabric et al., 2008; Galí et al., 2013).
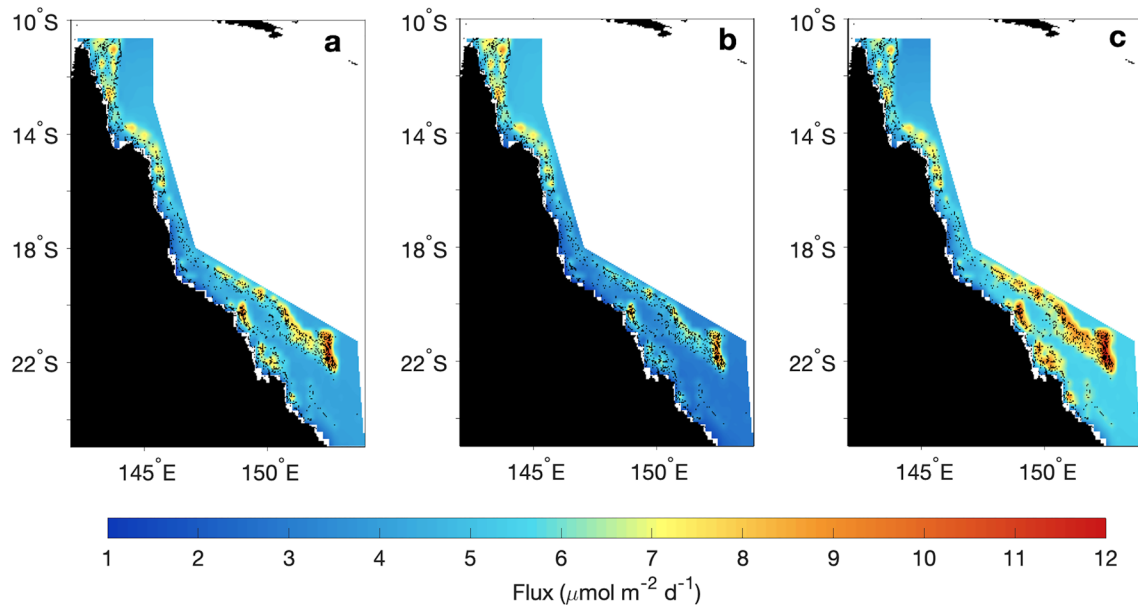
Figure 6. (a) Annual, (b) winter (May-October), and (c) summer (November-April) average DMS flux in the GBR. Values represent the average of the three DMS sea-air flux parameterizations calculated in this analysis. Northeastern Australia and the location of coral reefs in the GBRMP are shown in black. DMS, dimethylsulfide; GBR, Great Barrier Reef; GBRMP, Great Barrier Reef Marine Park.

The regression derived between DMS_w, SST, and PAR explained 71% of the variance in observed DMS_w. The resulting calculated DMS_w agrees with observed seasonal trends in the GBR (Jones et al., 2018), indicating that the regression predicts DMS_w reasonably well. The remaining variability was likely driven by nonlinear processes such as DMS(P) cycling by marine microbes (Bourne et al., 2016; Bullock et al., 2017; Sun et al., 2016), photolysis and vertical mixing in the water column (Gabric et al., 2008; Galí et al., 2013; Toole et al., 2003). The relative contribution of corals and marine algae to measured DMS_w cannot be quantified from this analysis. However, *Acropora* corals are the dominant coral genus throughout the GBR and are a relatively abundant source of DMSP for liberation of DMS to the coral reef environment (Swan et al., 2017a). DMS_w is often higher in seawater sampled directly over the coral reef compared to the lagoon (Jones et al., 2018) and so, corals likely contributed a large portion of measured DMS_w.
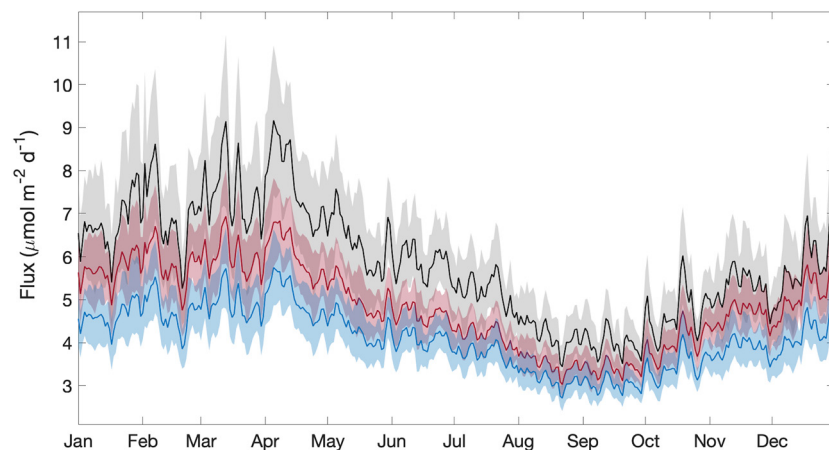

Figure 7. Climatology ±2 SE (shaded region) of DMS sea-air flux area-averaged over the GBR, calculated from the parameterization of Nightingale et al. (2000) (black), Goddijn-Murphy et al. (2012) (red), and Vlahos and Monahan (2009) (blue). SE, standard errors; DMS, dimethylsulfide; GBR, Great Barrier Reef.

The parameterization of DMS_w as a function of PAR at 5 m agrees with that of Vallina and Simó (2007), who derived a linear regression between DMS_w and solar radiation in the upper mixed layer. The relationship with solar radiation explained >90% of the variance in a global monthly climatology of DMS_w derived from the Global Seawater DMS database (Kettle et al., 1999). While Vallina and Simó (2007) suggested that SST is not an important predictor of DMS_w, the global DMS database contains very few DMS_w surveys close to a coral reef. In the southern GBR, PAR alone explained only ~30% of the variance in observed DMS_w and required a second predictor variable of SST to explain a significant portion of the variance in observed DMS_w. The importance of SST in predicting DMS_w likely reflects the significant impact of thermal stress on DMS production by corals and zooxanthellae (Raina et al., 2013). Although the range of measured SST was narrow (3.5 °C), laboratory studies have demonstrated that small changes in SST can significantly influence DMS production by corals (Deschaseaux et al., 2014b). Further research is needed to establish the validity of the GBR observed relationship between DMS_w, SST, and PAR in other coral reef systems.

The parameterization of DMS_w in coral reef seawaters as a function of SST and PAR is a simple approach and does not account for the impacts of other factors which may influence DMS biosynthesis such as ocean acidification and changes to coral reef ecosystem structure. Mesocosm experiments in the subtropical North Atlantic revealed a decrease in algal-derived DMS with lower pH due to reduced rates of microbial catabolism of DMSP (Archer et al., 2018). The same could be true of coral-derived DMS production, which is partially driven by microbial DMSP catabolism (Raina et al., 2009). Other studies have demonstrated that temperature has a stronger influence on DMS production in algae, where increased production in response to temperature outweighed the decline in biosynthesis due to acidification (Arnold et al., 2013). Ongoing coral reef degradation, due to coral bleaching, crown of thorns outbreaks and changing water quality may also affect DMS_w concentration in reef seawaters (discussed in Jackson et al. (2020)). A decline in coral-derived DMS_w could occur with reduced coral cover; however, DMS-producing marine algae can dominate degraded coral reef ecosystems (De'ath & Fabricius, 2010; McCook & Diaz-Pulido, 2002) and counteract a decline in coral-derived DMS production. Further research is required to determine the synergistic impacts of ocean warming, ocean acidification, and coral reef degradation on DMS(P) biosynthesis in coral reefs. Additional measurements of DMS_w in coral reef seawaters are also needed and will greatly improve the parameterization presented in this analysis. Nevertheless, the results provide insight into the source strength of coral reefs to the atmospheric sulfur budget.

Calculated DMS_w area-averaged over the GBR ranged from ~1 nmol L^{-1} in late winter to ~2.4 nmol L^{-1} in late summer (Figure 5a). Reported mean DMS_w concentrations for the GBR lagoon (deeper waters which surround the coral reef platforms) range from 0.8 nmol L^{-1} (0.6–1 nmol L^{-1}, $n = 4$) in winter to 1.9 nmol L^{-1} (0.1–3.4 nmol L^{-1}, $n = 224$) in summer (Jones et al., 2018). DMS_w is typically higher in shallow waters over the coral reef, ranging from 1.7 nmol L^{-1} (0.1–7.7 nmol L^{-1}, $n = 160$) in winter to 3.1 nmol L^{-1} (0.1–54 nmol L^{-1}, $n = 226$) in summer (Jones et al., 2018). The range of calculated DMS_w falls within the mean range reported for the GBR lagoon and coral reef waters. This was expected given that the RV *Investigator* data set is comprised of measurements taken both in the deeper lagoon and at several stations in shallower waters close to the coral reef (Figure 1). DMS_w calculated from the multiple linear regression derived from the RV *Investigator* data set may therefore underestimate concentrations over the coral reef (Figure 4).

The range of calculated DMS_w is ~1 nmol L^{-1} lower than that reported in the Lana et al. (2011) climatology for the Eastern Australian biogeochemical province (~2–4 nmol L^{-1}). The seasonal summer peak in DMS_w also occurs later in our climatology (February-March, rather than October), due to prescribing a maximum DMS_w value for days when SST exceeds the coral thermal stress threshold. Imposing an upper limit on DMS_w accounted for the effect of high SST and irradiance on coral and algal DMS production. High SST can reduce the PAR absorption capacity of algal photosystems, leading to excess production of ROS and oxidative damage in the coral holobiont (Lesser, 2006, 2011). DMS(P) scavenge ROS, forming DMSO, which results in a decline in ambient DMS_w concentration (Deschaseaux et al., 2014a; Fischer & Jones, 2012; Jones et al., 2007). The DMS_w climatology presented in this analysis may be closer to contemporary concentrations in the GBR after back-to-back coral bleaching events and the loss of up to ~40% of hard coral cover between March and November 2016 (Hughes et al., 2018). The RV *Investigator* sampled DMS_w in the GBR 8 months after the 2016 mass coral bleaching event and this may be one reason why measured DMS_w was lower than other studies have documented in the GBR (e.g., Jones et al., 2018).

Average DMS sea-air flux in the GBR ranged from $\sim$3 μmol m^{-2} d^{-1} in late winter to a maximum of $\sim$11 μmol m^{-2} d^{-1} in late summer (Figure 7). This estimate is similar in magnitude to that presented in Lana et al. (2011) for the Eastern Australian biogeochemical province ($\sim$5–15 μmol m^{-2} d^{-1}). Again, the seasonal peak in sea-air flux occurs later in summer in our climatology (February-March, rather than October), likely due to prescribing an upper limit on DMS$_w$ for SST beyond the coral thermal stress threshold. DMS flux was highest over the coral reef (Figure 6), due to the inclusion of a direct coral-atmosphere DMS flux estimate. Field-based findings have demonstrated that the southern GBR is a strong, albeit intermittent, source of DMS above the background oceanic signal (Jones et al., 2007; Swan et al., 2017b). However, there remains uncertainty in the source strength of direct coral-atmosphere DMS release.

Swan et al. (2017b) estimate that only 0.2 μmol m^{-2} d^{-1} is released from the coral reef, based on measurements of DMS$_a$ made at a fixed location at Heron Island (southern GBR). This is significantly lower than the estimate of $\sim$22 μmol m^{-2} d^{-1} provided by Hopkins et al. (2016), possibly due to difficulties in distinguishing the coral reef and oceanic DMS$_a$ sources under strong atmospheric mixing conditions from the prevailing southeasterly trade winds. The estimate provided by Hopkins et al. (2016) is the only direct measurement of coral-atmosphere DMS release; however, this estimate assumes that *Acropora* spp. are the sole source of direct coral-air DMS flux and does not account for variability in the extent of coral exposure or the complexity of the reef environment (Hopkins et al., 2016). Inclusion of this previously unaccounted for influence on DMS flux yields a more accurate estimate of the contribution of coral reefs to the atmospheric sulfur budget. Further research is needed to reduce the uncertainty in coral-air DMS flux and to accurately scale laboratory-derived fluxes to the natural coral reef environment.

We estimate that 0.03–0.05 Tg yr^{-1} of DMS is released from the GBR (0.02 Tg yr^{-1} of sulfur). This agrees with a previous estimate of 0.03 Tg yr^{-1} of DMS for the GBR lagoon and associated coral reefs, calculated from field measurements of DMS$_w$ over the past three decades (Jones et al., 2018). The range is slightly higher due to the inclusion of direct coral-atmosphere DMS release in our flux calculations. Assuming that DMS production and flux are constant across coral reefs, global tropical coral reefs ($\sim$600,000 km^2) could release 0.06–0.08 Tg yr^{-1} of DMS (0.03–0.04 Tg yr^{-1} of sulfur). Global sea-air flux is estimated to be 17.6–34.4 Tg yr^{-1} of sulfur in the form of DMS (Kettle & Andreae, 2000; Lana et al., 2011; Land et al., 2014). The contribution of sulfur as DMS from coral reefs represents 0.1–0.2% of global sea-air flux estimates, which is a disproportionate amount of sulfur released from $\sim$0.1% of the ocean surface (Spalding et al., 2001).

Global modeling studies have found that marine DMS is an important source of sulfate aerosol, influencing climate (Gabric et al., 2013; Mahajan et al., 2015; Thomas et al., 2010; Woodhouse et al., 2010) and providing a cooling effect of up to 0.45 °C (Fiddes et al., 2018). Given that coral reefs are strong regional sources of DMS, it is hypothesized that DMS emissions may influence the local radiative balance (Jackson et al., 2020; Jones et al., 2018; Swan et al., 2016) via a negative feedback on aerosol and cloud formation (e.g., Cropp et al., 2007). However, this coral reef source of atmospheric sulfur is not currently accounted for in global climatologies. Fiddes et al. (2020) was the first model study to explicitly account for the coral reef source of DMS by adding a laboratory-based estimate of 50 nmol to the Lana et al. (2011) DMS$_w$ climatology, scaled to the percentage of coral cover. This approach estimated that coral reefs release 0.3 Tg yr^{-1} of DMS (Fiddes et al., 2020), an order of magnitude higher than what is estimated by this study. Despite the high coral reef DMS flux estimate, Fiddes et al. (2020) found only a small response in nucleation and Aitken mode aerosol number concentrations and mass. This implies that coral reef DMS emissions are not important in contemporary regional climate, likely due to the dominance of anthropogenic, continental, and sea spray aerosols (Chen et al., 2019; Mallet et al., 2016). However, observational studies in the GBR suggest that DMS flux could influence local aerosol processes (Modini et al., 2009; Swan et al., 2016), which are perhaps not captured by global or regional climate models. Therefore, the importance of coral reef-derived DMS on the local radiative balance remains uncertain. Future work will test if the inclusion of coral reef-derived DMS in regional climatologies and regionally focused earth system models improves model accuracy and addresses the importance of coral reefs in biogeophysical processes.

5. Conclusions

This analysis supports previous findings that coral reefs are a significant regional source of DMS. The relationship between DMS_w, SST, and PAR is successfully parameterized and used to estimate the source strength of coral reefs to the sulfur cycle. The release of DMS from corals exposed to air at low tide is an important process that is not accounted for in current DMS sea-air flux calculations. By accounting for direct coral-atmosphere DMS release, we show that the total contribution of coral reefs is higher than previous estimates. Assuming that DMS production and sea-air flux are constant across coral reefs, 0.08 Tg yr^{-1} of DMS (0.04 Tg yr^{-1} of sulfur) could be released from tropical coral reefs, with the potential to influence the local radiative balance. This is the first parameterization of seawater DMS concentration in coral reefs and provides valuable insight into the role of coral reefs in global sulfur cycling.

Our DMS_w proxy can be used to investigate how changes to SST and PAR (due to changes in cloud cover and water clarity) might affect DMS production and flux from coral reefs in future. Ongoing ocean warming, acidification, and declining water quality are adversely affecting coral reef ecosystems and may lead to an ecological regime shift as coral resilience to disturbances continues to decline. This may lead to a change in DMS production and sea-air flux from coral reefs, with potential impacts on the local radiative balance.

Conflict of Interest

The authors declare no conflicts of interest.

Data Availability Statement

Underway measurements from Marine National Facility RV *Investigator* voyage IN2016_V05 (in2016_v05uwy5min_csv.zip) are available at url: https://www.marlin.csiro.au. Daily MODIS Aqua and Terra observations of SST, PAR, k490, and CHL are available from NASA's OceanColor Distributed Active Archive Centre (NASA Goddard Space Flight Center, 2018).

References

Anderson, J. M., Chow, W. S., & Park, Y. (1995). The grand design of photosynthesis: Acclimation of the photosynthetic apparatus to environmental cues. *Photosynthesis Research*, *46*(1–2), 129–139. https://doi.org/10.1007/BF00020423

Andreae, M. O. (1995). Climatic effects of changing atmospheric aerosol levels. *World Survey of Climatology*, *16*, 347–398.

Andreae, M. O., & Crutzen, P. J. (1997). Atmospheric aerosols: Biogeochemical sources and role in atmospheric chemistry. *Science*, *276*(5315), 1052–1058. https://doi.org/10.1126/science.276.5315.1052

Archer, S. D., Suffrian, K., Posman, K. M., Bach, L. T., Matrai, P. A., Countway, P. D., et al. (2018). Processes that contribute to decreased dimethyl sulfide production in response to ocean acidification in subtropical waters. *Frontiers in Marine Science*, *5*, 245. https://doi.org/10.3389/fmars.2018.00245

Arnold, H. E., Kerrison, P., & Steinke, M. (2013). Interacting effects of ocean acidification and warming on growth and DMS-production in the haptophyte coccolithophore *Emiliania huxleyi*. *Global Change Biology*, *19*(4), 1007–1016. https://doi.org/10.1111/gcb.12105

Bainbridge, S. J. (2017). Temperature and light patterns at four reefs along the Great Barrier Reef during the 2015-2016 Austral summer: Understanding patterns of observed coral bleaching. *Journal of Operational Oceanography*, *10*(1), 16–29. https://doi.org/10.1080/1755876X.2017.1290863

Berndt, T., Scholz, W., Mentler, B., Fischer, L., Hoffmann, E. H., Tilgner, A., et al. (2019). Fast peroxy radical isomerization and OH recycling in the reaction of OH radicals with dimethyl sulfide. *The Journal of Physical Chemistry Letters*, *10*(21), 6478–6483. https://doi.org/10.1021/acs.jpclett.9b02567

Bigg, E., & Turvey, D. (1978). Sources of atmospheric particles over Australia. *Atmospheric Environment*, *12*(8), 1643–1655.

Bourne, D. G., Morrow, K. M., & Webster, N. S. (2016). Insights into the coral microbiome: Underpinning the health and resilience of reef ecosystems. *Annual Review of Microbiology*, *70*, 317–340. https://doi.org/10.1146/annurev-micro-102215-095440

Broadbent, A. D., & Jones, G. B. (2006). Seasonal and diurnal cycles of dimethylsulfide, dimethylsulfoniopropionate and dimethylsulfoxide at One Tree Reef lagoon. *Environmental Chemistry*, *3*(4), 260–267. https://doi.org/10.1071/EN06011

Broadbent, A. D., Jones, G. B., & Jones, R. J. (2002). DMSP in corals and benthic algae from the Great Barrier Reef. *Estuarine, Coastal and Shelf Science*, *55*(4), 547–555. https://doi.org/10.1006/ecss.2002.1021

Buckee, J., Pattiaratchi, C., & Verduin, J. (2020). Partial mortality of intertidal corals due to seasonal daytime low water levels at the Houtman Abrolhos Islands. *Coral Reefs*, *39*, 537–543. https://doi.org/10.1007/s00338-019-01887-5

Bullock, H. A., Luo, H., & Whitman, W. B. (2017). Evolution of dimethylsulfoniopropionate metabolism in marine phytoplankton and bacteria. *Frontiers in Microbiology*, *8*, 637. https://doi.org/10.3389/fmicb.2017.00637

Carslaw, K. S., Lee, L. A., Reddington, C. L., Pringle, K. J., Rap, A., Forster, P. M., et al. (2013). Large contribution of natural aerosols to uncertainty in indirect forcing. *Nature*, *503*(7474), 67–71. https://doi.org/10.1038/nature12674

Chen, Z., Schofield, R., Rayner, P., Zhang, T., Liu, C., Vincent, C., et al. (2019). Characterization of aerosols over the Great Barrier Reef: The influence of transported continental sources. *Science of the Total Environment*, *690*, 426–437. https://doi.org/10.1016/j.scitotenv.2019.07.007

Christiansen, S., Salter, M. E., Gorokhova, E., Nguyen, Q. T., & Bilde, M. (2019). Sea spray aerosol formation: Laboratory results on the role of air entrainment, water temperature, and phytoplankton biomass. *Environmental Science and Technology*, *53*(22), 14107–13116. https://doi.org/10.1021/acs.est.9b04078

Copernicus Climate Change Service (C3S). (2019). *ERA5: Fifth generation of ECMWF atmospheric reanalysis of the global climate. Hourly u and v-wind speed components on single levels from 1979 to present*. Retrieved from https://cds.climate.copernicus.eu/cdsapp#!/home

Cropp, R., Gabric, A. J., van Tran, D., Jones, G. B., Swan, H. B., & Butler, H. (2018). Coral reef aerosol emissions in response to irradiance stress in the Great Barrier Reef, Australia. *Ambio*, *47*(6), 671–681. https://doi.org/10.1007/s13280-018-1018-y

Cropp, R., Norbury, J., & Braddock, R. (2007). Dimethylsulphide, clouds, and phytoplankton: Insights from a simple plankton ecosystem feedback model. *Global Biogeochemical Cycles*, *21*, GB2024. https://doi.org/10.1029/2006GB002812

Davis, K. A., Pawlak, G., & Monismith, S. G. (2020). Turbulence and coral reefs. *Annual Review of Marine Science*, *13*, 343–373. https://doi.org/10.1146/annurev-marine-042120-071823

De'ath, G., & Fabricius, K. (2010). Water quality as a regional driver of coral biodiversity and macroalgae on the Great Barrier Reef. *Ecological Applications*, *20*(3), 840–850. https://doi.org/10.1890/08-2023.1

Deschaseaux, E. S. M., Beltran, V., Jones, G. B., Deseo, M. A., Swan, H. B., Harrison, P. L., & Eyre, B. D. (2014a). Comparative response of DMS and DMSP concentrations in Symbiodinium clades C1 and D1 under thermal stress. *Journal of Experimental Marine Biology and Ecology*, *459*, 181–189. https://doi.org/10.1016/j.jembe.2014.05.018

Deschaseaux, E. S. M., Hardefeldt, J., Jones, G. B., & Reichelt-Brushett, A. (2018). High zinc exposure leads to reduced dimethylsulfoniopropionate (DMSP) levels in both the host and endosymbionts of the reef-building coral Acropora aspera. *Marine Pollution Bulletin*, *126*, 93–100. https://doi.org/10.1016/j.marpolbul.2017.10.070

Deschaseaux, E. S. M., Jones, G. B., Deseo, M. A., Shepherd, K. M., Kiene, R. P., Swan, H. B., et al. (2014b). Effects of environmental factors on dimethylated sulfur compounds and their potential role in the antioxidant system of the coral holobiont. *Limnology and Oceanography*, *59*(3), 758–768. https://doi.org/10.4319/lo.2014.59.3.0758

Downs, C. A., Fauth, J. E., Halas, J. C., Dustan, P., Bemiss, J., & Woodley, C. M. (2002). Oxidative stress and seasonal coral bleaching. *Free Radical Biology and Medicine*, *33*(4), 533–543. https://doi.org/10.1016/S0891-5849(02)00907-3

Fiddes, S. L., Woodhouse, M. T., Lane, T. P., & Schofield, R. (2020). Coral reef-derived dimethyl sulfide and the climatic impact of the loss of coral reefs. *Atmospheric Chemistry and Physics Discussions*, 1–29. https://doi.org/10.5194/acp-2020-1054

Fiddes, S. L., Woodhouse, M. T., Nicholls, Z., Lane, T. P., & Schofield, R. (2018). Cloud, precipitation and radiation responses to large perturbations in global dimethyl sulfide. *Atmospheric Chemistry and Physics*, *18*(14), 10177–10198. https://doi.org/10.5194/acp-18-10177-2018

Fischer, E., & Jones, G. B. (2012). Atmospheric dimethylsulphide production from corals in the Great Barrier Reef and links to solar radiation, climate and coral bleaching. *Biogeochemistry*, *110*(1–3), 31–46. https://doi.org/10.1007/s10533-012-9719-y

Gabric, A. J., Matrai, P., Jones, G. B., & Middleton, J. (2018). The nexus between sea ice and polar emissions of marine biogenic aerosols. *Bulletin of the American Meteorological Society*, *99*(1), 61–81. https://doi.org/10.1175/BAMS-D-16-0254.1

Gabric, A. J., Matrai, P., Kiene, R. P., Cropp, R., Dacey, J., DiTullio, G., et al. (2008). Factors determining the vertical profile of dimethylsulfide in the Sargasso Sea during summer. *Deep Sea Research Part II: Topical Studies in Oceanography*, *55*(10–13), 1505–1518. https://doi.org/10.1016/j.dsr2.2008.02.002

Gabric, A. J., Qu, B., Rotstayn, L., & Shephard, J. M. (2013). Global simulations of the impact on contemporary climate of a perturbation to the sea-to-air flux of dimethylsulfide. *Australian Meteorological and Oceanographic Journal*, *63*(3), 365–376.

Galí, M., Simó, R., Vila-Costa, M., Ruiz-González, C., Gasol, J. M., & Matrai, P. (2013). Diel patterns of oceanic dimethylsulfide (DMS) cycling: Microbial and physical drivers. *Global Biogeochemical Cycles*, *27*, 620–636. https://doi.org/10.1002/gbc.20047

Gardner, S. G., Nielsen, D. A., Laczka, O., Shimmon, R., Beltran, V. H., Ralph, P. J., & Petrou, K. (2016). Dimethylsulfoniopropionate, superoxide dismutase and glutathione as stress response indicators in three corals under short-term hyposalinity stress. *Proceedings of the Royal Society B*, *283*(1824), 20152418. https://doi.org/10.1098/rspb.2015.2418

Goddijn-Murphy, L., Woolf, D. K., & Marandino, C. (2012). Space-based retrievals of air-sea gas transfer velocities using altimeters: Calibration for dimethyl sulfide. *Journal of Geophysical Research*, *117*, C08028. https://doi.org/10.1029/2011JC007535

Gondwe, M., Krol, M., Gieskes, W., Klaassen, W., & De Baar, H. (2003). The contribution of ocean-leaving DMS to the global atmospheric burdens of DMS, MSA, SO$_2$, and NSS SO$_4^=$. *Global Biogeochemical Cycles*, *17*(2), 1056. https://doi.org/10.1029/2002GB001937

Gorbunov, M. Y., Kolber, Z. S., Lesser, M. P., & Falkowski, P. G. (2001). Photosynthesis and photoprotection in symbiotic corals. *Limnology and Oceanography*, *46*(1), 75–85. https://doi.org/10.4319/lo.2001.46.1.0075

Guibert, I., Bourdreux, F., Bonnard, I., Pochon, X., Dubousquet, V., Raharivelomanana, P., et al. (2020). Dimethylsulfoniopropionate concentration in coral reef invertebrates varies according to species assemblages. *Scientific Reports*, *10*, 9922. https://doi.org/10.1038/s41598-020-66290-5

Hill, R. W., Dacey, J., & Edward, A. (2000). Dimethylsulfoniopropionate in giant clams (Tridacnidae). *The Biological Bulletin*, *199*(2), 108–115. https://doi.org/10.2307/1542870

Hopkins, F. E., Bell, T. G., Yang, M., Suggett, D. J., & Steinke, M. (2016). Air exposure of coral is a significant source of dimethylsulfide (DMS) to the atmosphere. *Scientific Reports*, *6*, 36031. https://doi.org/10.1038/srep36031

Hughes, T. P., Kerry, J. T., Baird, A. H., Connolly, S. R., Dietzel, A., Eakin, C. M., et al. (2018). Global warming transforms coral reef assemblages. *Nature*, *556*(7702), 492–496. https://doi.org/10.1038/s41586-018-0041-2

IPCC. (2014). In Core Writing Team, R. K. Pachauri, & L. A. Meyer (Eds.), *Climate change 2014: Synthesis report. Contribution of working Groups I, II and III to the fifth assessment report of the intergovernmental panel on climate change*. Geneva, Switzerland: IPCC.

Jackson, R. L., Gabric, A. J., & Cropp, R. (2018). Effects of ocean warming and coral bleaching on aerosol emissions in the Great Barrier Reef, Australia. *Scientific Reports*, *8*(1), 14048. https://doi.org/10.1038/s41598-018-32470-7

Jackson, R. L., Gabric, A. J., Woodhouse, M. T., & Cropp, R. (2020). Dimethylsulfide (DMS), marine biogenic aerosols and the ecophysiology of coral reefs. *Biogeosciences*, *17*, 2181–2204. https://doi.org/10.5194/bg-17-2181-2020

Johnson, M. T., Hughes, C., Bell, T. G., & Liss, P. S. (2011). A Rumsfeldian analysis of uncertainty in air-sea gas exchange. In S. Komori, W. McGillism, & R. Kurose (Eds.), *Gas transfer at water surfaces 2010* (pp. 464–484). Kyoto, Japan: Kyoto University Press.

Jones, G. B., Curran, M., & Broadbent, A. (1994). Dimethylsulfide in the South Pacific. In O. Bellwood, H. Choat, & N. Saxena (Eds.), *Recent advances in marine science and technology* (pp. 183–190). Townsville: James Cook University of North Queensland.

Jones, G. B., Curran, M., Broadbent, A., King, S., Fischer, E., & Jones, R. (2007). Factors affecting the cycling of dimethylsulfide and dimethylsulfoniopropionate in coral reef waters of the Great Barrier Reef. *Environmental Chemistry*, *4*(5), 310–322. https://doi.org/10.1071/EN06065

Jones, G. B., Curran, M., Deschaseaux, E. S. M., Omori, Y., Tanimoto, H., Swan, H. B., et al. (2018). The flux and emission of dimethylsulfide from the Great Barrier Reef region and potential influence on the climate of NE Australia. *Journal of Geophysical Research: Atmospheres*, *123*, 13835–13856. https://doi.org/10.1029/2018JD029210

Jones, G. B., & King, S. (2015). Dimethylsulphoniopropionate (DMSP) as an indicator of bleaching tolerance in scleractinian corals. *Journal of Marine Science and Engineering*, *3*(2), 444–465. https://doi.org/10.3390/jmse3020444

Jones, R. J., Hoegh-Guldberg, O., Larkum, A. W., & Schreiber, U. (2002). Temperature-induced bleaching of corals begins with impairment of the CO_2 fixation mechanism in zooxanthellae. *Plant, Cell and Environment*, *21*(12), 1219–1230. https://doi.org/10.1046/j.1365-3040.1998.00345.x

Jones, R. J., Ward, S., Amri, A. Y., & Hoegh-Guldberg, O. (2000). Changes in quantum efficiency of photosystem II of symbiotic dinoflagellates of corals after heat stress, and of bleached corals sampled after the 1998 Great Barrier Reef mass bleaching event. *Marine and Freshwater Research*, *51*(1), 63–71.

Kameyama, S., Tanimoto, H., Inomata, S., Tsunogai, U., Ooki, A., Yokouchi, Y., et al. (2009). Equilibrator inlet-proton transfer reaction-mass spectrometry (EI-PTR-MS) for sensitive, high-resolution measurement of dimethyl sulfide dissolved in seawater. *Analytical Chemistry*, *81*, 9021–9026. https://doi.org/10.1021/ac901630h

Kettle, A. J., & Andreae, M. O. (2000). Flux of dimethylsulfide from the oceans: A comparison of updated data sets and flux models. *Journal of Geophysical Research*, *105*(D22), 26793–26808. https://doi.org/10.1029/2000JD900252

Kettle, A. J., Andreae, M. O., Amouroux, D., Andreae, T. W., Bates, T. S., Berresheim, H., et al. (1999). A global database of sea surface dimethyl sulfide (DMS) measurements and a procedure to predict sea surface DMS as a function of latitude, longitude, and month. *Global Biogeochemical Cycles*, *13*(2), 399–344. https://doi.org/10.1029/1999GB900004

Kloster, S., Feichter, J., Maier-Reimer, E., Six, K. D., Stier, P., & Wetzel, P. (2006). DMS cycle in the marine ocean-atmosphere system-a global model study. *Biogeosciences*, *3*(1), 29–51.

Korhonen, H., Carslaw, K. S., Spracklen, D. V., Mann, G. W., & Woodhouse, M. T. (2008). Influence of oceanic dimethyl sulfide emissions on cloud condensation nuclei concentrations and seasonality over the remote Southern Hemisphere oceans: A global model study. *Journal of Geophysical Research*, *113*, D15204. https://doi.org/10.1029/2007JD009718

Lana, A., Bell, T., Simó, R., Vallina, S., Ballabrera-Poy, J., Kettle, A., et al. (2011). An updated climatology of surface dimethyl sulfide concentrations and emission fluxes in the global ocean. *Global Biogeochemical Cycles*, *25*, GB1004. https://doi.org/10.1029/2010GB003850

Lana, A., Simó, R., Vallina, S., & Dachs, J. (2012). Potential for a biogenic influence on cloud microphysics over the ocean: A correlation study with satellite-derived data. *Atmospheric Chemistry and Physics*, *12*(17), 7977–7993. https://doi.org/10.5194/acp-12-7977-2012

Land, P. E., Shutler, J. D., Bell, T., & Yang, M. (2014). Exploiting satellite earth observation to quantify current global oceanic DMS flux and its future climate sensitivity. *Journal of Geophysical Research: Oceans*, *119*, 7725–7740. https://doi.org/10.1002/2014JC010104

Leck, C., & Bigg, E. K. (2008). Comparison of sources and nature of the tropical aerosol with the summer high Arctic aerosol. *Tellus B: Chemical and Physical Meteorology*, *60*(1), 118–126. https://doi.org/10.1111/j.1600-0889.2007.00315.x

Lesser, M. P. (2006). Oxidative stress in marine environments: Biochemistry and physiological ecology. *Annual Review of Physiology*, *68*, 253–278. https://doi.org/10.1146/annurev.physiol.68.040104.110001

Lesser, M. P. (2011). Coral bleaching: Causes and mechanisms. In Z. Dubinsky, & N. Stambler (Eds.), *Coral reefs: An ecosystem in transition* (pp. 405–419). Dordrecht: Springer.

Liss, P. S., & Slater, P. G. (1974). Flux of gases across the air-sea interface. *Nature*, *247*, 181–184.

Liu, G., Strong, A. E., Skirving, W., & Arzayus, L. F. (2006). Overview of NOAA Coral Reef Watch program's near-real time satellite global coral bleaching monitoring activities. Paper presented at the *Proceedings of the 10th International Coral Reef Symposium*. Okinawa, Japan.

Long, M. S., Keene, W. C., Kieber, D. J., Frossard, A. A., Russell, L. M., Maben, J. R., et al. (2014). Light-enhanced primary marine aerosol production from biologically productive seawater. *Geophysical Research Letters*, *41*, 2661–2670. https://doi.org/10.001/2014GL059436

Mahajan, A. S., Fadnavis, S., Thomas, M. A., Pozzoli, L., Gupta, S., Royer, S., et al. (2015). Quantifying the impacts of an updated global dimethyl sulfide climatology on cloud microphysics and aerosol radiative forcing. *Journal of Geophysical Research: Atmospheres*, *120*, 2524–2536. https://doi.org/10.1002/2014JD022687

Mallet, M., Cravigan, L., Miljevic, B., Vaattovaara, P., Descaseaux, E. S. M., Swan, H. B., et al. (2016). Sea spray aerosol in the Great Barrier Reef and the presence of nonvolatile organics. *Journal of Geophysical Research: Atmospheres*, *121*, 7088–7099. https://doi.org/10.1002/2016jd024966

McCook, L. J., & Diaz-Pulido, G. (2002). The fate of bleached corals: Patterns and dynamics of algal recruitment. *Marine Ecology Progress Series*, *232*, 115–128. https://doi.org/10.3354/meps232115

McGillis, W., Dacey, J., Frew, N., Bock, E., & Nelson, R. (2000). Water-air flux of dimethylsulfide. *Journal of Geophysical Research*, *105*(C1), 1187–1193. https://doi.org/10.1029/1999JC900243

McParland, E. L., & Levine, N. M. (2019). The role of differential DMSP production and community composition in predicting variability of global surface DMSP concentrations. *Limnology and Oceanography*, *64*(2), 757–773. https://doi.org/10.1002/lno.11076

Melis, A. (1999). Photosystem-II damage and repair cycle in chloroplasts: What modulates the rate of photodamage in vivo? *Trends in Plant Science*, *4*(4), 130–135.

Middleton, J. H., Coutis, P., Griffith, D. A., Macks, A., McTaggart, A., Merrifield, M., & Nippard, G. J. (1994). Circulation and water mass characteristics of the southern Great Barrier Reef. *Marine and Freshwater Research*, *45*(1), 1–18. https://doi.org/10.1071/MF9940001

Modini, R. L., Ristovski, Z., Johnson, G. R., He, C., Surawski, N., Morawska, L., et al. (2009). New particle formation and growth at a remote, sub-tropical coastal location. *Atmospheric Chemistry and Physics*, *9*(19), 7607–7621. https://doi.org/10.5194/acp-9-7607-2009

NASA Goddard Space Flight Center, Ocean Ecology Laboratory, Ocean Biology Processing Group. (2018). *Moderate-Resolution Imaging Spectroradiometer (MODIS) Aqua and Terra Data; 2018 Reprocessing*.

Nightingale, P. D., Malin, G., Law, C. S., Watson, A. J., Liss, P. S., Liddicoat, M. I., et al. (2000). In situ evaluation of air-sea gas exchange parameterizations using novel conservative and volatile tracers. *Global Biogeochemical Cycles*, *14*(1), 373–387. https://doi.org/10.1029/1999GB900091

Omori, Y., Tanimoto, H., Inomata, S., Ikeda, K., Iwata, T., Kameyama, S., et al. (2017). Sea-to-air flux of dimethyl sulfide in the South and North Pacific Ocean as measured by proton transfer reaction-mass spectrometry coupled with the gradient flux technique. *Journal of Geophysical Research: Atmospheres*, *122*, 7216–7231. https://doi.org/10.1002/2017JD026527

Przyjazny, A. W., Janicki, W., Chrzanowski, W., & Staszewki, R. (1983). Headspace gas chromatographic determination coefficients of selected organosulphur compounds and their dependence of some parameters. *Journal of Chromatography*, *280*, 249–260. https://doi.org/10.1016/S0021-9673(00)91567-X

Raina, J., Tapiolas, D. M., Forêt, S., Lutz, A., Abrego, D., Ceh, J., et al. (2013). DMSP biosynthesis by an animal and its role in coral thermal stress response. *Nature*, *502*(7473), 677–680. https://doi.org/10.1038/nature12677

Raina, J., Tapiolas, D. M., Willis, B. L., & Bourne, D. G. (2009). Coral-associated bacteria and their role in the biogeochemical cycling of sulfur. *Applied and Environmental Microbiology*, *75*(11), 3492–3501. https://doi.org/10.1128/AEM.02567-08

Rosic, N., Remond, C., & Mello-Athayde, M. A. (2020). Differential impact of heat stress on reef-building corals under different light conditions. *Marine Environmental Research*, *158*, 104947. https://doi.org/10.1016/j.marenvres.2020.104947

Saltzman, E., King, D., Holmen, K., & Leck, C. (1993). Experimental determination of the diffusion coefficient of dimethylsulfide in water. *Journal of Geophysical Research*, *98*(C9), 16481–16486. https://doi.org/10.1029/93JC01858

Sanchez, K. J., Chen, C., Russell, L. M., Betha, R., Liu, J., Price, D. J., et al. (2018). Substantial seasonal contribution of observed biogenic sulfate particles to cloud condensation nuclei. *Scientific Reports*, *8*(1), 3235. https://doi.org/10.1038/s41598-018-21590-9

Schwarzenbach, R. P., Gschwend, P. M., & Imboden, D. M. (1994). *Environmental organic chemistry*. New York, NY: John Wiley.

Skirving, W. J., Enríquez, S., Hedley, J., Dove, S., Eakin, C., Mason, R., et al. (2018). Remote sensing of coral bleaching using temperature and light: Progress towards an operational algorithm. *Remote Sensing*, *10*(1), 18. https://doi.org/10.3390/rs10010018

Spalding, M., Ravilious, C., & Green, E. P. (2001). *World Atlas of coral reefs*. University of California Press.

Spiese, C. E., Kieber, D. J., Nomura, C. T., & Kiene, R. P. (2009). Reduction of dimethylsulfoxide to dimethylsulfide by marine phytoplankton. *Limnology and Oceanography*, *54*(2), 560–570. https://doi.org/10.4319/lo.2009.54.2.0560

Stefels, J. (2000). Physiological aspects of the production and conversion of DMSP in marine algae and higher plants. *Journal of Sea Research*, *43*(3–4), 183–197. https://doi.org/10.1016/S1385-1101(00)00030-7

Sun, J., Todd, J. D., Thrash, J. C., Qian, Y., Qian, M. C., Temperton, B., et al. (2016). The abundant marine bacterium *Pelagibacter* simultaneously catabolizes dimethylsulfoniopropionate to the gases dimethyl sulfide and methanethiol. *Nature Microbiology*, *1*(8), 16065. https://doi.org/10.1038/NMICROBIOL.2016.65

Sunda, W., Kieber, D. J., Kiene, R. P., & Huntsman, S. (2002). An antioxidant function for DMSP and DMS in marine algae. *Nature*, *418*, 317–320.

Swan, H. B., Crough, R. W., Vaattovaara, P., Jones, G. B., Deschaseaux, E. S. M., Eyre, B. D., et al. (2016). Dimethyl sulfide and other biogenic volatile organic compound emissions from branching coral and reef seawater: Potential sources of secondary aerosol over the Great Barrier Reef. *Journal of Atmospheric Chemistry*, *73*(3), 303–328. https://doi.org/10.1007/s10874-016-9327-7

Swan, H. B., Deschaseaux, E. S. M., Jones, G. B., & Eyre, B. D. (2017a). The relative abundance of dimethylsulfoniopropionate (DMSP) among other zwitterions in branching coral at Heron Island, southern Great Barrier Reef. *Analytical and Bioanalytical Chemistry*, *409*(18), 4409–4423. https://doi.org/10.1007/s00216-017-0385-8

Swan, H. B., Jones, G. B., Deschaseaux, E. S., & Eyre, B. D. (2017b). Coral reef origins of atmospheric dimethylsulfide at Heron Island, southern Great Barrier Reef, Australia. *Biogeosciences*, *14*(1), 229–239. https://doi.org/10.5194/bg-14-229-2017

Thomas, M. A., Suntharalingam, P., Pozzoli, L., Rast, S., Devasthale, A., Kloster, S., et al. (2010). Quantification of DMS aerosol-cloud-climate interactions using the ECHAM5-HAMMOZ model in a current climate scenario. *Atmospheric Chemistry and Physics*, *10*, 7425–7438. https://doi.org/10.5194/acp-10-7425-2010

Toole, D. A., Kieber, D. J., Kiene, R. P., Siegel, D. A., & Nelson, N. B. (2003). Photolysis and the dimethylsulfide (DMS) summer paradox in the Sargasso Sea. *Limnology and Oceanography*, *48*(3), 1088–1100. https://doi.org/10.4319/lo.2003.48.3.1088

Twomey, S. (1974). Pollution and the planetary albedo. *Atmospheric Environment (1967)*, *8*(12), 1251–1256.

Vallina, S. M., & Simó, R. (2007). Strong relationship between DMS and the solar radiation dose over the global surface ocean. *Science*, *315*(5811), 506–508. https://doi.org/10.1126/science.1133680

Veres, P. R., Neuman, J. A., Bertram, T. H., Assaf, E., Wolfe, G. M., Williamson, C. J., et al. (2020). Global airborne sampling reveals a previously unobserved dimethyl sulfide oxidation mechanism in the marine atmosphere. *Proceedings of the National Academy of Sciences of the United States of America*, *117*(9), 4505–4510. https://doi.org/10.1073/pnas.1919344117

Vlahos, P., & Monahan, E. C. (2009). A generalized model for the air-sea transfer of dimethyl sulfide at high wind speeds. *Geophysical Research Letters*, *36*, L21605. https://doi.org/10.1029/2009GLO40695

Weis, V. M. (2008). Cellular mechanisms of Cnidarian bleaching: Stress causes the collapse of symbiosis. *Journal of Experimental Biology*, *211*(19), 3059–3066. https://doi.org/10.1242/jeb.009597

Wild, C., Huettel, M., Klueter, A., Kremb, S. G., Rasheed, M. Y., & Jørgensen, B. (2004). Coral mucous functions as an energy carrier and particle trap in the reef ecosystem. *Nature*, *428*, 66–70. https://doi.org/10.1038/nature02344

Winters, G., Loya, Y., Röttgers, R., & Beer, S. (2003). Photoinhibition in shallow-water colonies of the coral *Stylophora pistillata* as measured in situ. *Limnology and Oceanography*, *48*(4), 1388–1393. https://doi.org/10.4319/lo.2003.48.4.1388

Woodhouse, M. T., Carslaw, K. S., Mann, G. W., Vallina, S. M., Vogt, M., Halloran, P. R., & Boucher, O. (2010). Low sensitivity of cloud condensation nuclei to changes in the sea-air flux of dimethyl-sulphide. *Atmospheric Chemistry and Physics*, *10*(16), 7545–7559. https://doi.org/10.5194/acp-10-7545-2010

Woodhouse, M. T., Mann, G., Carslaw, K. S., & Boucher, O. (2013). Sensitivity of cloud condensation nuclei to regional changes in dimethyl-sulphide emissions. *Atmospheric Chemistry and Physics*, *13*(5), 2723–2733. https://doi.org/10.5194/acp-13-2723-2013

Yakovleva, I. M., Baird, A. H., Yamamoto, H. H., Bhagooli, R., Nonaka, M., & Hidaka, M. (2009). Algal symbionts increase oxidative damage and death in coral larvae at high temperatures. *Marine Ecology Progress Series*, *378*, 105–112. https://doi.org/10.3354/meps07857